Shahrood University of Technology

Journal of Mining and Environment (JME)

Journal homepage: www.jme.shahroodut.ac.ir

Iranian Society of Mining Engineering (IRSME)

Effect of Stable Nano-microbubbles on Sulfide Copper Flotation and Reduction of Chemicals Dosage

Ali Nikouei Mahani[1], Mohammad Karamoozian[1], Mohammad Jahani Chegeni[1]*, and Mohammad Mahmoodi Meymand[2]

1. Faculty of Mining, Petroleum & Geophysics Engineering, Shahrood University of Technology, Shahrood, Iran.
2. Research and Development Division, Sarcheshmeh Copper Mine, National Iranian Copper Industries Company, Rafsanjan, Iran

Article Info

Received 1 June 2023
Received in Revised form 11 July 2023
Accepted 16 July 2023
Published online 16 July 2023

DOI: 10.22044/jme.2023.13205.2413

Keywords

Stable nano-microbubbles
Interaction
Experiment design
Chemicals dosage
Recovery

Abstract

Generally, mineral processing plants generate a large quantity of waste in the form of fine particles. The flotation speed of mineral microbubbles by coarse bubbles is dramatically higher than that of individual particles. The advantage of microbubbles is due to the increase of binding efficiency of conventional bubbles with fine particles coated with microbubbles. Here, the focus is on reducing chemicals consumption and improving recovery. After preparing a representative sample, XRF, XRD, and mineralogical analyses were performed. Then 50 experiments were selected by experimental design using the response surface method (RSM), and in the form of central Composite design (CCD) by (design expert) DX 13 software. The interactions of collector consumption, frother agent, pH, particle size, and solid percentage were investigated, and 25 experiments using typical flotation and without nano-microbubbles and others with nano-microbubbles were conducted. The laboratory standard limit of the collector used in the pilot plant of the Sarcheshmeh Copper copper complex is 40 g/t (25 g/t of C7240 plus 15 g/t of Z11). Here, by consuming 20 g/t of collector in the absence of nanomicrobubbles, a recovery of 79.96% and in the presence of nanomicrobubbles, a recovery of 80.07% was obtained, that is a 50% reduction in collector consumption and a 0.11% increase in recovery was observed. Also the laboratory standard limit of frother used in the pilot plant of Sarcheshemeh Copper Complex is 30 g/t (15 g/t of MIBC plus 15 g/t of A65). Here, by using 10 g/t of frother in the absence of nanomicrobubbles, a recovery of 78.12%, and in the presence of nanomicrobubbles, a recovery of 82.05% was obtained. In other words, a decrease of 66.6% in the consumption of frother and an increase of 1.93% in recovery was observed.

1. Introduction

The minimum degree of hydration required for flotation of a particle depends on its size. The entrainment factor is also considered as an important contributing mechanism in the recovery of fine particles which, when combined with the low actual flotation rate, can explain much of the observed behavior of such fines. Ahmed and Jameson reported the flotation rate of fine particles, less than 50 microns in diameter, and showed that the flotation rate is strongly affected by the bubble size. The effects of particle density and impeller speed were also investigated [2]. The probability of foam collection increases rapidly with decreasing bubble size [3]. The low

✉ *Corresponding author: m.jahani1983@gmail.com (M. Jahani Chegeni)*

probability of bubble and particle collision is the main reason for low flotation efficiency for fine and ultra-fine particles [4-9]. Specific laboratory tests with fines (mostly at the subsieve size range) are presented as examples by Matis *et al*. They concluded that although froth flotation is a common selective separation process in mineral processing, it becomes inefficient for beneficiating fines [10]. Mining industries jointly create a lot of waste in the form of fine and fine particles [11]. Dissolved gas bubbles can significantly improve the flotation performance [12]. Maoming *et al*. indicated that nanobubble increased P_2O_5 recovery by up to 10%~30% for a given Acid Insoluble (A.I.) rejection, depending on the characteristic of phosphate samples. They also showed that nanobubbles almost doubled the coarse phosphate flotation rate constant and increased the flotation selectivity index by up to 25%. [13]. Using nanobubbles in the flotation tank of mechanical cells and column flotation improved the flotation recovery by 27% ~ 8% in a specific product grade [14]. For coarse particles, the reasons for recovery can be related to the highly turbulent nature of pulp in a normal flotation cell. To improve recovery, it is necessary to find a way to contact particles and bubbles in a static environment. A new process for the flotation of coarse particles is described in which a fluidized bed was created in the flotation cell and the flow conditions were very mild, and the high concentration of solids resulted in rapid adsorption of the particles [15]. The presence of nano-sized particles was detected through dynamic light scattering for days, when pure oxygen was used to generate the bubbles, and for less than 1 h, in the case of air bubbles. Furthermore, the zeta potential measured in the water after the introduction of oxygen micro- and nanobubbles was in the range from −45 mV to −34 mV and from −20 mV to −17 mV in water bubbled with air, indicating the presence of stable electrically charged particles. This study suggested a strong possibility of the existence of nanobubbles in water for a long time. [16]. Fine particles have a low collision efficiency with gas bubbles and float slowly. There are a large sum of research works aimed at overcoming the inefficient collision of small particles with rising air bubbles. Miettinen *et al.* dealt with the review of the influence of bubble size, particle aggregation, different flow conditions, particle induction time, as well as the action of surface and capillary forces on fine particle–bubble capture [17]. Albijanic *et al.* indicated that there is a relationship between the time of the collected concentrate, the copper grade of the sample, and the time of the bubbles connecting to the particles as well as the measurements are more sensitive to the amount of unreleased material. The fast-floating material was higher grade, with a lower attachment time indicating that the measured bubble–particle attachment time could be used to characterize flotation performance of an ore [18]. There is a high non-linear correlation between mineral liberation, copper grade, collector dosage, and attachment time [19]. Calgaroto *et al.* indicated that a reduction in pressure makes the super-saturated liquid suffers cavitation and nanobubbles are generated. Medium pH and solutions tested were adjusted, in the air saturation vessel, before the nanobubbles were formed, and this allowed to control (*in situ*) the surface charge/zeta potential-size of the forming nanobubbles. Accordingly, the sizes of the nanobubbles depended on their charge and increased with pH. Thus charged and uncharged stable nanobubbles can be tailor-made with or without surfactants and it is expected that their use will broaden options in mineral flotation especially if collectors coated nanobubbles (‘‘bubble-collectors’’) were employed [20]. Ahmadi *et al.* showed that with the passage of time, the average dimensions of nano-microbubbles increase due to the decrease in the amount of dissolved oxygen in water and also the decrease in the absolute value of the surface zeta potential [21]. Leistner *et al.* indicated that ultrafine magnetite can be recovered similar to fine magnetite when the gangue particles are fine as well. In contrast, fine magnetite recovery drops significantly when ultrafine quartz is used as the gangue mineral system [22]. The flotation speed of mineral microbubbles by coarse bubbles is several times compared of the flotation speed of individual particles [23]. The presence of nanobubbles improves quartz flotation by 21% in dimensions (+106-425 microns) [24]. de Medeiros and Baltar suggested using long chain collectors for the flotation of fines [25]. Tao and Sobhy indicated hydrophobicity of particles and nanobubbles produced on the surface of the

particles by affecting the balance between hydrodynamic and chemical forces of the surface that guide the movement of the particle moving around the surface of the bubble, increase the process of interaction between the particles and the bubble [26]. Ebrahimi *et al*. showed simultaneous use of two factors stable nanobubbles and ultrasonic waves under irradiation can improve the yield of coarse (−850 + 420 μm), medium (−420 + 105 μm) and fine (−105 μm) particles by more than 10%, 10%, and 30%, respectively [27]. Farrokhpay *et al*. stated that the advantage of microbubbles may be attributed to a higher attachment efficiency of the conventional bubbles with the fine particles covered with microbubbles [28]. In another study, Farrokhpay *et al*. stated that the problem of fine particle flotation is mainly due to their low collision and attachment efficiencies with bubbles [29]. Li *et al*. concluded that nanobubbles are responsible for the improved flotation performance of coal particles [30]. Chang *et al*. showed that oxidized coal flotation in the presence of nanobubbles resulted in 10% higher combustible matter recovery than conventional air bubble flotation [31]. Nanobubble flotation has emerged as a promising process for increasing the flotation efficiency of ultra-fine particles in recent years [32-36]. The basic mechanisms of flotation of fine particles with nanobubbles are very interesting and have attracted much attention in recent research works [37, 38].

The common optimization method of a multivariable system follows one factor at a time, and its main defect is neglecting the interaction between factors. Therefore, it does not mean the complete effect of various factors on the process [39-45]. Further, this approach requires more data to determine the optimal level, which is a time-consuming and unwanted process [46]. Accordingly, design of experiments (DOE) can be used to optimize such multivariable systems, as its successful use has been proven by many researchers in mineral processing [47-50]. Response surface modeling (RSM) is one of the effective methods of DOE, which includes a combination of mathematical and statistical methods based on a multivariate non-linear model in which all factors are varied in a set of experiments. This approach is a valuable, cost-effective and practical tool for analyzing processes and quantifying the relationship between controllable inputs and response levels (outputs), which is obtained even in the presence of complex interactions [39, 40, and 51-53]. Generally, the process of response surface methodology includes five main steps: (1) designing a series of experiments, (2) developing a mathematical model with the best fit for the functional relationship between input and output factors, (iii) finding the optimal set of experimental factors that produce the maximum or minimum value of the response(s), (iv) predicting the response(s) and checking the model's capability in a set of experiments, and (v) desplaying the direct and interactive effects of the factors [50 -53]. This method includes various designs such as Central Composite Design (CCD), Box-Benchken Design (BBD), three-level factorial, and Doehlert. Among them, CCD is one of the most popular designs used in process optimization [39, 40, and 53]. It is known that CCDs with fractional factorial points are the best option for building statistical models in terms of the number of tests required and the quality of the obtained data [54].

In a CCD, the range of trials (N) is decided in keeping with Equation (1):

$$N = 2^{(n-p)} + 2n + n_c \quad (1)$$

where n is the number of factors and p is a fraction of the number of factors (p = 0 for a full factorial design), n_c is the number of central runs to estimate the experimental error, and 2n represents the axial runs. In addition, all the factors are studied at five levels (-α, -1, 0, +1, +α), where the α value is the star (axial) point and is measured by the following formula [53, 55, and 56]:

$$\alpha = (2^{(n-p)})^{\frac{1}{4}} \quad (2)$$

Two important models, including the first-order model (Equation 3) and the second-order polynomial model (Equation 4), are usually used in the RSM method.

$$Y = \beta_0 + \sum_{i=1}^{K} \beta_i x_i + \varepsilon \quad (3)$$

$$Y = \beta_0 + \sum_{i=1}^{K} \beta_i x_i + \sum_{i=1}^{k} \beta_{ii} x_i^2 + \sum_{1 \le i \le j}^{k} \beta_{ij} x_i x_j + \varepsilon \quad (4)$$

where Y is the predicted response, k is the number of factors, and β_0 is a constant term. Also β_i indicates linear coefficients and x_i indicates variables or independent factors. Also β_{ii} represents quadratic coefficients, β_{ij} represents interaction coefficients, and ε represents error. In this research work, the experimental data have been statistically analyzed using the design expert software, and the factors with coded values are analyzed for uniform comparison according to the following equation:

$$x_i = \frac{X_i - X_0}{\Delta X} \quad (5)$$

where x_i means the dimensionless encoded value of factor i, X_i represents the actual value of the coefficient, and X_0 represents the value of X_i at the center point and ΔX is the step change value [49].

In this research work, the main goal is to investigate the effect of stable nano-microbubbles on reducing the chemicals dosage in flotation process of the copper sulfide sample of Sarcheshmeh Copper Complex.

2. Materials and Methods

2.1. Sampling

At first, a representative sample weighing 200 kg was taken from the input feed conveyor to the milling unit of the concentration plant No. 1 of the Sarcheshmeh Copper Complex. The target sample was crushed in two jaw crushers, one with a fixed jaw and the other with a movable jaw, and using a vibrating screen (10 mesh) or (2 mm) all the particles reached into less than 2 mm. From the general sample, after mixing and homogenization, samples weighing 1000 grams were prepared for comminution and flotation tests. Also representative samples were taken from the general samples for XRD and XRF analyses.

2.2. Chemical analysis

The percentage of elements and some types of compounds available in the sample were determined by XRF analysis method. The results of XRF analysis of the sample are shown in Table 1. The obtained results indicate that the amount of copper in the feed is 0.62% and the amount of copper oxide is 4.84%.

Table 1. XRF analysis of copper sulfide ore of Sarcheshmeh Copper Mine

Chemical formula	Cu	CuO	Fe_2O_3	Fe	S	K_2O	MgO	SiO_2	Al_2O_3
%	0.62	0.03	10.10	7.07	3.37	3.27	2.18	53.43	17.34
Chemical formula	CaO	Na_2O	ZnO	TiO_2	Mo				
%	0.85	0.81	0.10	0.80	0.030				

Also the samples were sent to Sarcheshmeh Copper Complex laboratory for XRD analysis, and according to the analysis results, which are shown in Table 2, the main minerals in the sample were according to the below table:

Table 2. XRD test results.

Compound	Chemical formula	Content (%)
Quartz	SiO_2	14.1
Illite	$KAl_2(Si_3Al)O_{10}(OH)_2$	23
	$(K.H_3O)(Al.Mg.Fe)_2(Si.Al)_4O_{10}[(OH_2).(H_2O)]$	
Clinochlore	$(Mg.Fe^{2+})_5Al(Si_3Al)O_{10}(OH)_8$	8.3
	$Mg_5Al(AlSi_3O_{10})(OH)_8$	
Albite	$Na(AlSi_3O_8)$	3.9
Muscovite	$[KAl_2(AlSi_3O_{10})(FOH)_2]$	26.5
	$[(KF)_2(Al_2O_3)(SiO_2)_6(H_2O)]$	
Chamosite	$(Fe^{2+}.Mg.Fe^{3+})_5Al(Si_3Al)O_{10}(OH.O)_8$	9.4
	$(Fe^{2+},Mg,Al,Fe^{3+})_6(Si,Al)_4O_{10}(OH,O)_8$	
Pyrite	FeS_2	9.5
Amorph	-	5.2

2.3. Design of experiments

To perform flotation experiments, the response surface method (RSM) with the central composite design type (CCD) was used in the design expert 13 (DX13) software. The test conditions for five 5-level factors and one qualitative factor which is a nanobubble are listed in Table 3. A total of 50 experiments were obtained, of which 25 experiments were performed under normal conditions and 25 experiments were performed under nanobubble conditions. All items are listed in Table 3.

Table 3. Test conditions using DX13 software.

Factors	Name	-2	-1	0	1	2
A	Collector dosage (g/t)	20	25	40	45	50
B	Frother dosage (g/t)	10	15	30	40	50
C	pH	11.4	11.6	11.8	12	12.2
D	Particle size (µm)	38	11	75	53	106
E	Solid percent (%)	24	26	28	30	32
F	Nanobubble (mL)	-	-	0	1	-

Mechanical flotation tests were performed in a Denver laboratory flotation cell with a volume of 2.3 liters. Lime was also used to adjust the pH. Based on the initial optimization experiments, the solid percentage was 28%, the impeller speed was 1100 rpm, and pH = 11.8. First, the powdered samples were poured into the flotation cell and after two minutes of preparation and pH adjustment, the collector and frother were added to the cell. The preparation time of the collector and frother maker was considered to be 2 and 1 minutes, respectively. After that, aeration started, and frothing action was done in 12 minutes. The particle size in these experiments was selected in five dimensional ranges, which are included in Table 4, and their comminution time by the laboratory ball mill is also included in the same table. Pulp density in the mill was considered 50% by weight. Flotation pulp densities were determined in five different weight percents in the experiments, which are: 24, 26, 28, 30, and 32%. The collectors used for this series of laboratory tests were C7240 and Z11. For this reason, their values were different in each experiment but its laboratory standard in the pilot plant was 40 g/t. Also, gasoil was used as a co-collector for

molybdenum flotation, the constant amount of which was 13 g/t. Also two types of frothers, MIBC and A65, were used as variables in these tests, but its standard laboratory value in the pilot plant was 30 g/t. At the end, the rotor engine speed of the Denver laboratory flotation device was set to 1100 rpm. In addition, the water used in normal tests was urban drinking water.

The names of the chemicals used in the experiments are given in Table 5.

Table 4. Optimal times of different dimensional domains.

Sample number	1	2	3	4	5
Particle size (μm)	106	75	53	38	11
Optimal time	4′:18″	6′:19″	7′:27″	7′:29″	34′:53″

Table 5. Types of chemicals used in experiments.

Chemicals	Role of chemicals
Lime (CaO)	pH regulator
Polypropylene glycol - methyl ether (A65)	Frother
Methyl isobutyl carbinol (MIBC)	Frother
Sodium isopropyl xanthate (Z11)	Collector
(C7240)*	Collector
Gasoil	Co-collector

2.4. Nanobubble solution

The desired nanobubble maker device was equipped and built based on the phenomenon of hydrodynamic cavitation in Shahrood University of Technology. The nanobubble maker device consists of three main parts (air or gas inlet), applying pressure on the air and water mixture, pressure reduction or pressure drop zone, and releasing part of the dissolved air. The purpose of entering air into the nan-bubble maker device is to increase the solubility of air dissolved in water in order to increase the efficiency of the cavitation phenomenon, as well as bubble production. As a result, air or gas is injected in this device before the pump. The feature of the construction and design of this device is the use of several micro-nanobubble hydrodynamic generators with different throat diameters at the same time. It is worth mentioning that three generators were used in the nanobubble maker device designed in Shahrood University of Technology. Another unique feature of nanobubbles produced by this device is their stability for several days (months) in water [57]. To determine the dimensions of nanobubbles, a 1-day sample is placed in the Nano Particle Size Analyzer. This device works with the dynamic light diffraction method and also has the ability to measure the dimensions of particles in the range of 1 nanometer to 6 microns. The Cumulant method draws conclusions based on 3 parameters: number, volume, and intensity of samples. For these experiments, the refractive index of light was assumed to be 1.56 for nan-bubbles and 1.33 for water. Also the distribution of nano-scale particles was measured by laser light with a wavelength of 657 nm and a power of 50%. Based on the conducted experiments, the approximate size of the smallest and largest bubbles was 26.92 and 3091.11 nm, respectively. Figures 1, 2, and 3, respectively, show the distribution of bubbles based on three parameters: intensity, volume, and number. Figure 1, which is the distribution of nanobubbles based on intensity, had a normal distribution, and Figure 3, which is the distribution of nanobubbles based on number, had a lognormal distribution.

* A mixture of 10-20 wt % sodium alkyl dithiophosphate and 20-30 wt% sodium mercaptobenzothiozile

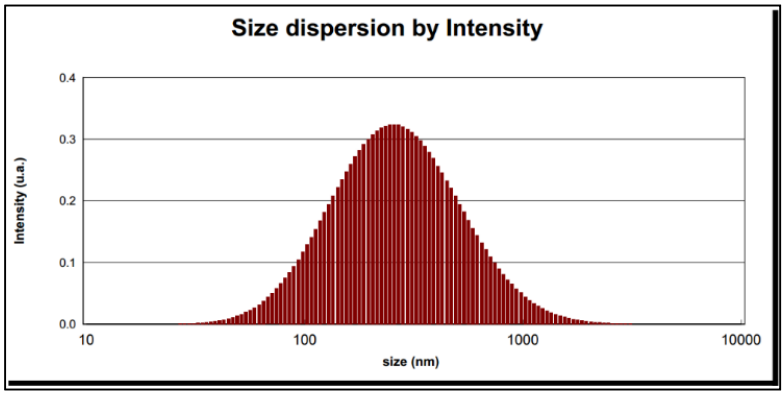

Figure 1. Distribution of nanobubbles based on intensity.

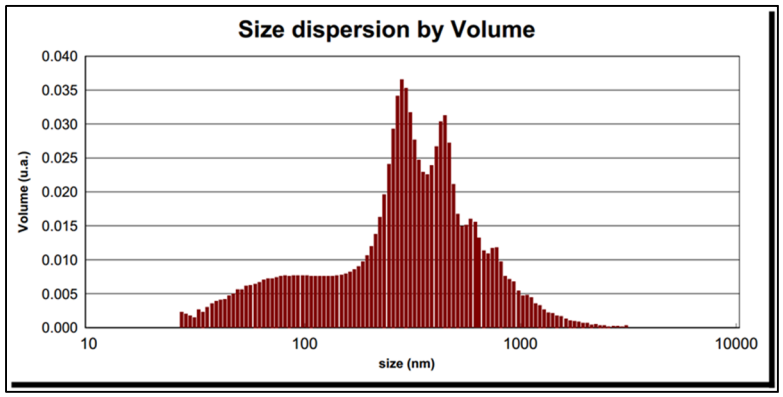

Figure 2. Distribution of nanobubbles based on volume.

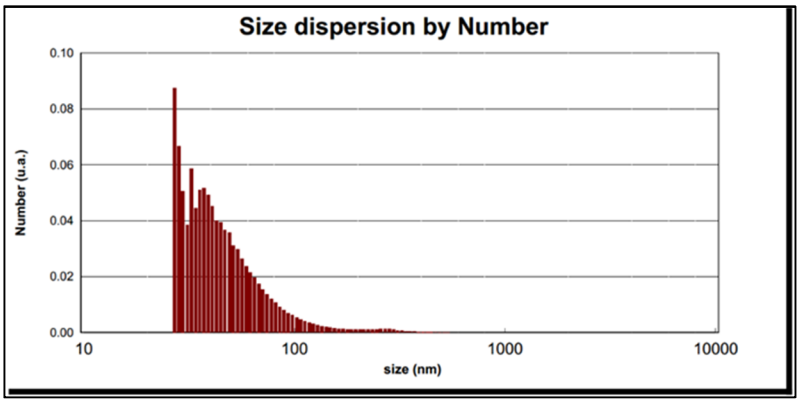

Figure 3. Distribution of nanobubbles based on number.

3. Results and Discussion

After performing the tests in two normal modes and with nano-microbubble, the samples were placed in the oven. After drying and weighing the samples, they were sent to the central laboratory of Sarcheshmeh Copper Complex. The results obtained are shown in Table 6.

Table 6. Design of experiments by response surface method.

Test number	Run	A: Collector (g/t)	B: Frother (g/t)	C: pH	D: Particle size (µm)	E: Solid percent (%)	F: Nano-bubble	Cu recovery (%)	Cu grade (%)	Cu: Separation efficiency (%)
1	19	25	15	11.6	11	30	0	85.8	5.01	76.92
2	36	45	15	11.6	11	26	0	92.2	3.12	75.66
3	42	25	40	11.6	11	26	0	92.2	3.24	76.25
4	39	25	15	12	11	26	0	86	4.59	76.21
5	16	45	15	12	11	30	0	92.6	8.3	86.6
6	6	25	40	12	11	30	0	90.4	2.34	69.01
7	28	25	15	11.6	53	26	0	75.1	3.7	65.56
8	7	45	15	11.6	53	30	0	74.2	3.3	63.69
9	49	25	40	11.6	53	30	0	84.9	3.93	73.7
10	29	45	40	11.6	53	26	0	90.1	5.38	81.02
11	44	25	40	12	53	26	0	89.6	8.31	83.95
12	38	45	40	12	53	26	0	88.6	5.76	80.36
13	3	20	30	11.8	75	28	0	84.9	10.51	80.87
14	4	50	30	11.8	75	28	0	83.8	7.59	78.18
15	26	40	10	11.8	75	28	0	76.2	7.46	71.37
16	32	40	50	11.4	75	28	0	85.7	5.48	77.58
17	47	40	30	12.2	75	28	0	84.6	4.56	75.01
18	11	40	30	11.8	75	28	0	86.6	9.06	81.67
19	33	40	30	11.8	38	28	0	85.8	5.19	77.18
20	10	40	30	11.8	106	28	0	85.4	6.76	78.89
21	25	40	30	11.8	75	24	0	89.9	6.39	82.34
22	21	40	30	11.8	75	32	0	87.2	5.17	78.34
23	20	40	30	11.8	75	28	0	88.2	7.92	82.37
24	48	40	30	11.8	75	28	0	87.3	5.23	78.43
25	35	40	30	11.8	75	28	0	85.5	6.3	78.48
26	8	25	15	11.6	11	30	1	86.1	4.36	75.76
27	14	45	15	11.6	11	26	1	92.6	8.63	86.82
28	46	25	40	11.6	11	26	1	79.7	5.42	72.6
29	45	25	15	12	11	26	1	86.8	6.9	80.3
30	40	45	15	12	11	30	1	92.6	8.66	86.84
31	37	25	40	12	11	30	1	85.3	6.9	79.01
32	50	25	15	11.6	53	26	1	74.1	4.7	66.91
33	43	45	15	11.6	53	30	1	71.1	5.28	64.86
34	9	25	40	11.6	53	26	1	82.5	6.75	76.29
35	34	45	40	11.6	53	26	1	86.6	8.53	81.4
36	30	25	40	12	53	26	1	89.5	10.72	85.15
37	2	45	40	12	53	28	1	88.3	7.06	81.72
38	23	20	30	11.8	75	28	1	86.5	9.35	81.81
39	15	50	30	11.8	75	28	1	85.3	7.17	79.21
40	22	40	10	11.8	75	28	1	76.2	8.08	71.63
41	17	40	50	11.8	75	28	1	84.1	6.06	76.99
42	5	40	30	11.4	75	28	1	88.3	6.75	81.45
43	18	40	30	12.2	75	28	1	85.2	7.7	79.57
44	24	40	30	11.8	38	28	1	87	6.05	79.48
45	41	40	30	11.8	106	24	1	83.2	4.36	73.52
46	31	40	30	11.8	75	32	1	84.2	5.69	76.6
47	27	40	30	11.8	75	28	1	86.9	6.4	79.84
48	12	40	30	11.8	75	28	1	87.1	5.5	78.81
49	13	40	30	11.8	75	28	1	88.8	5.67	81.08
50	1	40	30	11.8	75	26	1	85.5	6.21	78.4

3.1. Variance analysis for copper recovery

The statistical parameters of the analysis of variance (ANOVA) table, such as mean square, sum of square, variance ratio for all factors and each response level were calculated in the software. Here, 95% confidence was considered for the response level. For tests, in the (ANOVA) section, probability value values smaller than (0.05) indicate that the considered parameters are significant. The F-value here was equal to 6.07, which shows that the model is significant. Also the P-values smaller than 0.05 show that the expressions of the model are significant. If the P-values are greater than (0.1), they show that the parameters of the model are not significant. In this test, the parameters (A, B, C, AB, AC, AD, AE, BC, BD, BE, BF, CD, CE, DE, A^2, B^2, D^2) of the model are significant. The value of Lack of Fit showed 4.27, which means that the lack of fit is meaningless compared to the net error. 0.0577% is also likely that Lack of Fit is caused by disturbances. Finally, it is good to have a lack of fit because our model should be fit. Table 7 shows the analysis of variance for copper recovery.

Table 7. Analysis of variance for copper recovery.

Source	SS	DF	MS	F- value	p-value	
model	1050.03	26	40.39	6.07	< 0.0001	significant
A-Collector	72.28	1	72.28	10.87	0.0032	
B-Frother	39.60	1	39.60	5.96	0.0228	
C-pH	43.05	1	43.05	6.47	0.0181	
D-Particle size	4.22	1	4.22	0.6339	0.4341	
E-Solid percent	1.70	1	1.70	0.2561	0.6176	
F-Nano bubble	18.75	1	18.75	2.82	0.1066	
AB	82.37	1	82.37	12.39	0.0018	
AC	25.92	1	25.92	3.90	0.0605	
AD	40.67	1	40.67	6.12	0.0212	
AE	139.52	1	139.52	20.98	0.0001	
AF	0.1541	1	0.1541	0.0232	0.8803	
BC	24.99	1	24.99	3.76	0.0649	
BD	164.04	1	164.04	24.67	< 0.0001	
BE	117.44	1	117.44	17.66	0.0003	
BF	29.34	1	29.34	4.41	0.0468	
CD	86.25	1	86.25	12.97	0.0015	
CE	108.64	1	108.64	16.34	0.0005	
CF	12.22	1	12.22	1.84	0.1884	
DE	106.76	1	106.76	16.06	0.0006	
DF	9.78	1	9.78	1.47	0.2376	
EF	2.70	1	2.70	0.4062	0.5302	
A^2	41.33	1	41.33	6.22	0.0203	
B^2	144.64	1	144.64	21.75	0.0001	
C^2	3.58	1	3.58	0.5387	0.4704	
D^2	30.28	1	30.28	4.55	0.0437	
E^2	3.74	1	3.74	0.5622	0.4610	
Residual	152.93	23	6.65			
Lack of Fit	143.58	18	7.98	4.27	0.0577	Not significant
Pure error	9.35	5	1.87			
Cor Total	1202.96	49				

3.2. Statistical characteristics of results

The closer R^2 is to 1, the better, which here is 0.8729 for copper recovery, which is acceptable in statistics. "Adeq Precision" measures the signal to noise ratio which compares the range of predicted values in the design points to the average prediction error. A ratio greater than 4 is desirable, and here the number 10.6336 is obtained, which indicates a sufficient signal.

Equations 6 to 8 respectively show the models provided by Design Expert software for the recovery, grade, and separation efficiency of Sarcheshmeh copper ore.

Recovery = + 88.93 - 4.41 * A + 2.78 * B + 2.71 * C + 1.01 * D -0.5029 * E -0.6474 * F - 11.68 * AB + 5.16 * AC + 8.54 * AD - 18.69 * AE + 0.1036 * AF + 5.08 * BC + 20.86 * BD - 18.41 * BE - 1.61 * BF - 15.16 * CD + 23.55 * CE + 1.19 * CF + 17.62 * DE + 0.846 * DF + 0.5248 * EF - 4.32 * A^2 -7.07 * B^2 - 1.15 * C^2 - 5.83 * D^2 - 1.15 * E^2, R^2=0.8729, Adj R^2=0.7292, Pred R^2=0.2175	(6)
Grade = + 6.60 - 1.64 * A - 0.6254 * B + 1.33 * C + 1.59 * D - 0.3640 * E + 0.4026 * F - 0.8455 * AB - 0.9710 * AC - 1.88 * AD - 2.26 * AE + 0.2213 * AF - 0.9033 * BC + 0.8519 * BD - 4.30 * BE + 0.4841 * BF -1.74 * CD + 1.53 * CE - 0.0118 * CF + 1.86 * DE - 1.15 * DF - 0.0910 * EF, R^2= 0.6134, Adj R^2=0.3234, Pred R^2= - 0.3854	(7)
Separation Efficiency = + 82.03 - 5.81 * A + 1.03 * B + 3.79 * C + 3.29 * D - 1.20 * E + 0.3469 * F - 13.14 * AB + 5.67 * AC + 8.89 * AD - 20.68 * AE + 0.2199 * AF + 2.91 * BC + 23.80 * BD - 24.03 * BE - 0.3109 * BF - 17.68 * CD + 25.80 * CE + 0.9351 * CF + 19.94 * DE - 1.59 * DF + 0.6467 * EF - 3.14 * A^2 - 6.92 * B^2 -1.99 * C^2 - 9.06 * D^2 - 2.26 * E^2, R^2= 0.7943, Adj R^2= 0.5618, Pred R^2= - 0.4344	(8)

Since our goal was to reduce the chemicals dosage and increase recovery, for this reason, we did not consider the grade and separation efficiency. In other words, the goal and desire of Sarchesmeh Copper Complex from this research work was only the first goal which it was shown that this goal can be achieved with the interaction of stable nano-microbubble and frother. Therefore, in the following figures until the end of the article, only the graphs related to recovery are presented and analyzed.

The adequacy of the generated prediction model to recover more copper from the residual normal probability diagram is shown in Figure 4b. The data presented in Figure 4b follow a straight line exactly, which shows that there is no need to transform the real data. It can be concluded that the deviation between the predicted and experimental values is normally distributed and the proposed model fits the data well. This further supports the validity of the second-order model for predicting copper recovery.

3.3. Comparison of effect of all parameters on copper recovery in absence and presence of nano-microbubbles

Figure 5 shows the effect of all parameters on copper recovery in the absence of nano-microbubbles. In this figure, the parameters of the collector, frother, and particle size have the highest slope, which indicates the great impact of these three parameters on copper recovery in the absence of nano-microbubbles.

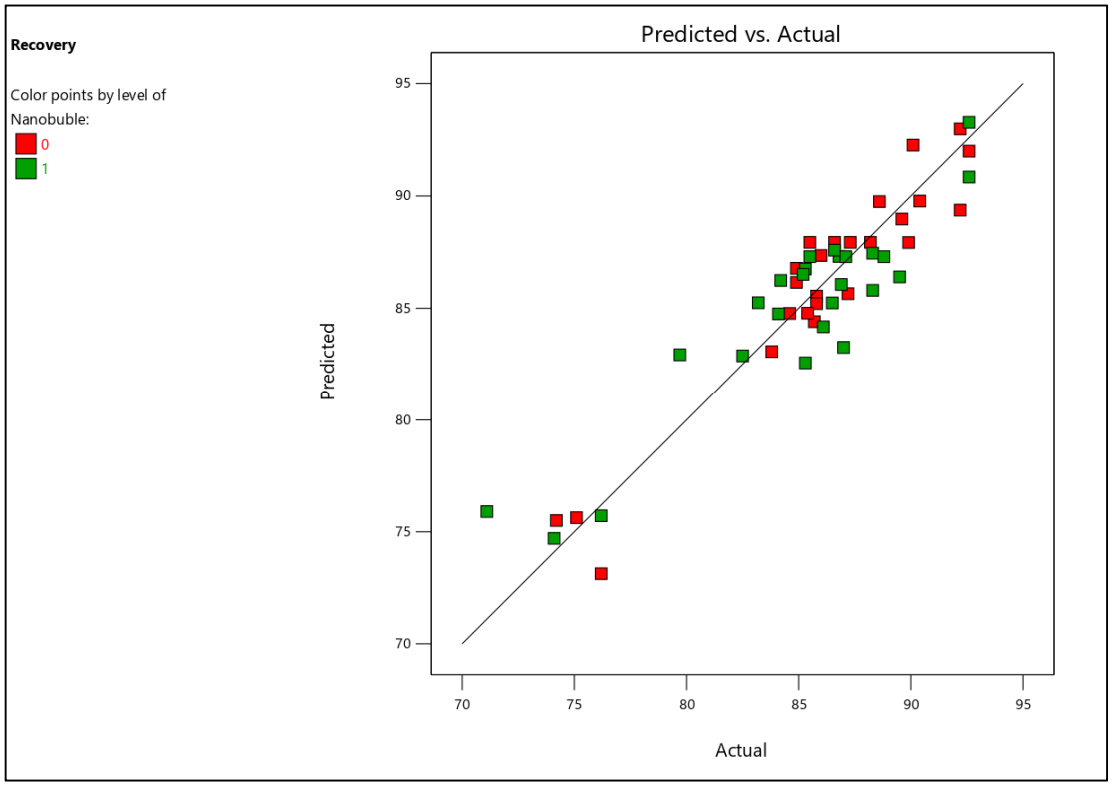

(a)

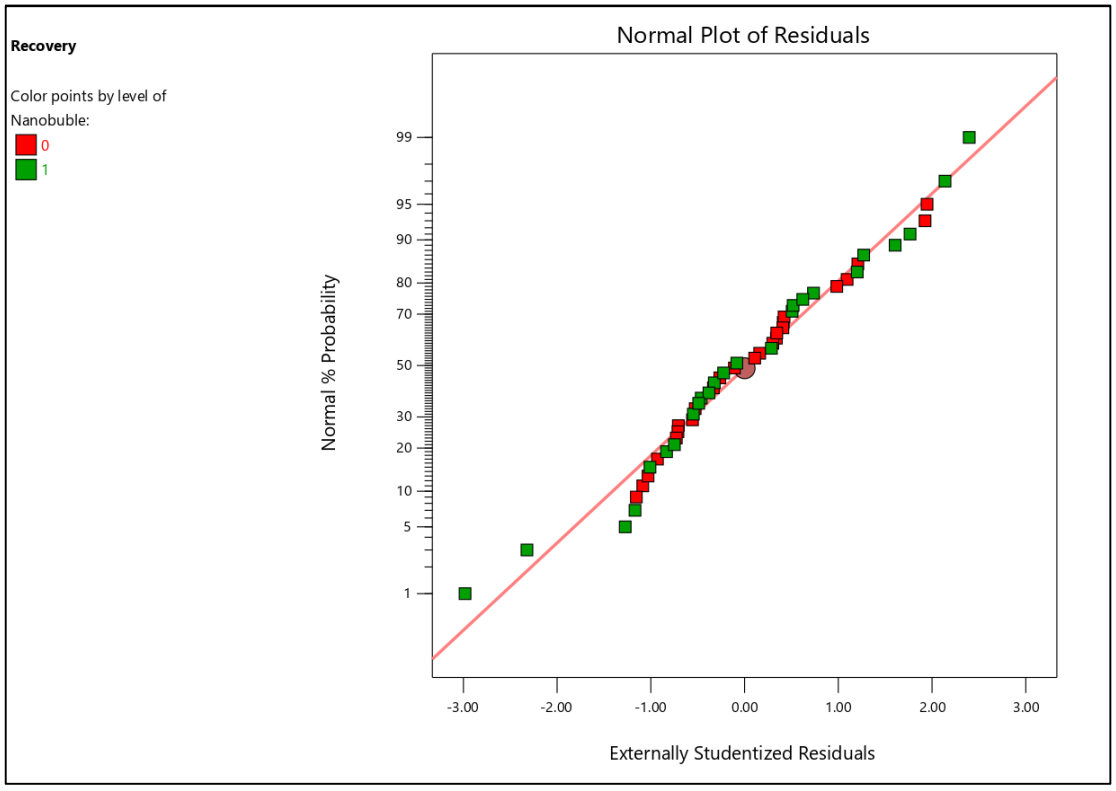

(b)

Figure 4. Plot of actual (measured) versus predicted values for copper recovery in (a) rougher flotation process and (b) normal probability versus studentized residual plot.

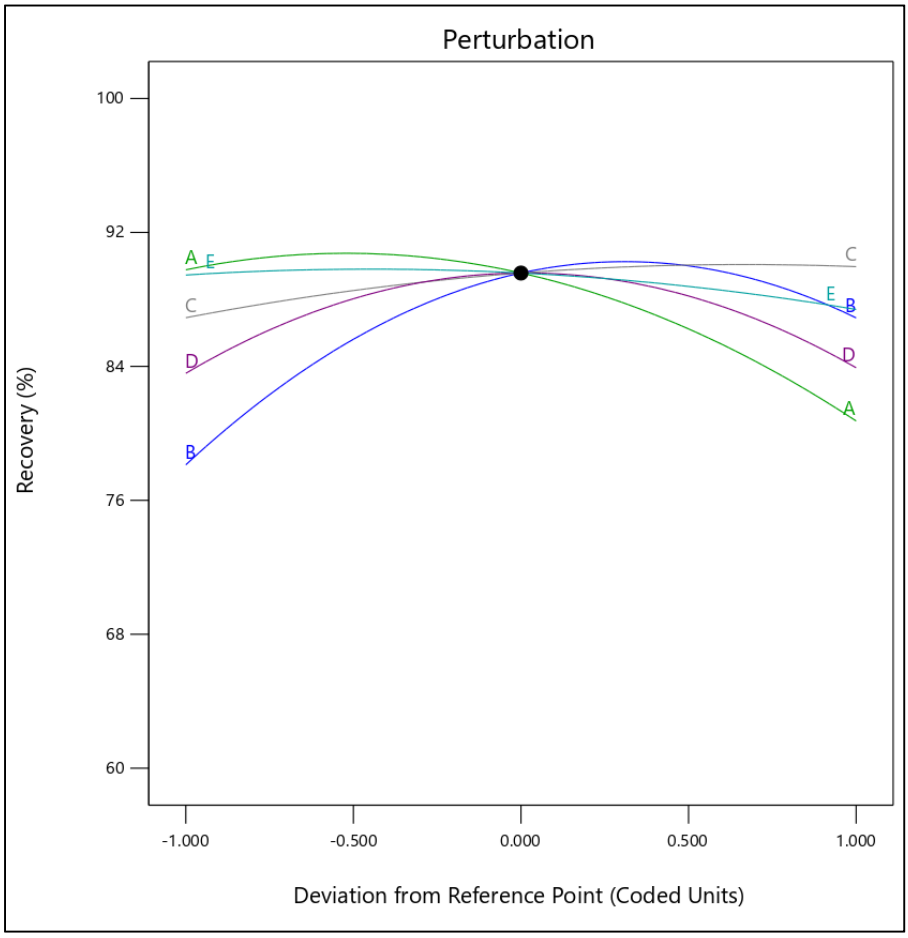

Figure 5. Effect of parameters on copper recovery in the absence of nano-microbubbles.

Figure 6 shows the effect of all parameters on copper recovery in the presence of nano-microbubbles. In this figure, the parameters collector, frother, and pH have the highest slope, which shows the great effect of these three parameters on copper recovery in the presence of nano-microbubbles. By comparing the two graphs (Figures 5 and 6), it can be understood that in the presence of nano-microbubbles, an increase in recovery was observed by reducing the amount of frother agent. By increasing the pH in the presence of nano-microbubbles, the recovery value increased compared to the absence of nano-microbubbles. The noteworthy point of these two graphs is that with the increase in particle size in the presence of nano-microbubbles, the amount of recovery also increased.

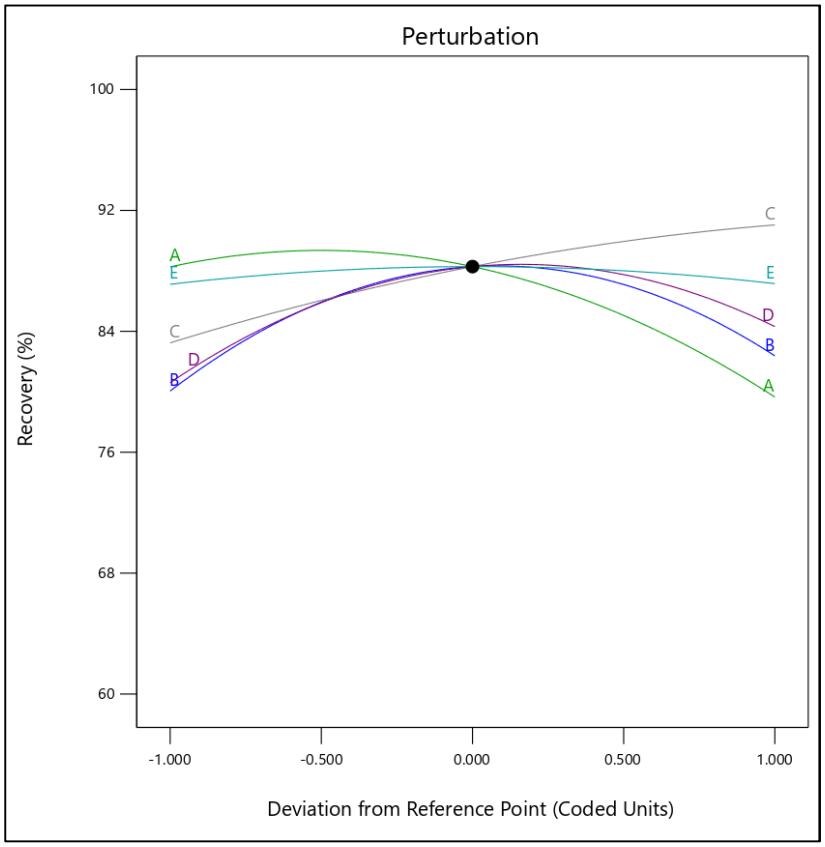

Figure 6. Effect of parameters on copper recovery in the presence of nano-microbubbles.

3.3.1. Effect of collector on recovery in presence and absence of nano-microbubbles

In the absence of nano-microbubbles in Figure 7, with the consumption of a 20 g⁄t collector, 79.96% recovery was observed and in the presence of nano-microbubbles, the recovery value was 80.07%, that is a 0.11% increase was recorded in the presence of nano-microbubbles. The standard consumption limit of the pilot plant of Sarcheshmeh Copper Complex for the collector dosage is 40 g⁄t, and here such a result was obtained with 50% less consumption. One of the remarkable results is that the recovery can be increased by using less collector in the presence of nano-microbubble, the reason is that nano-microbubble is also used as a secondary collector [58].

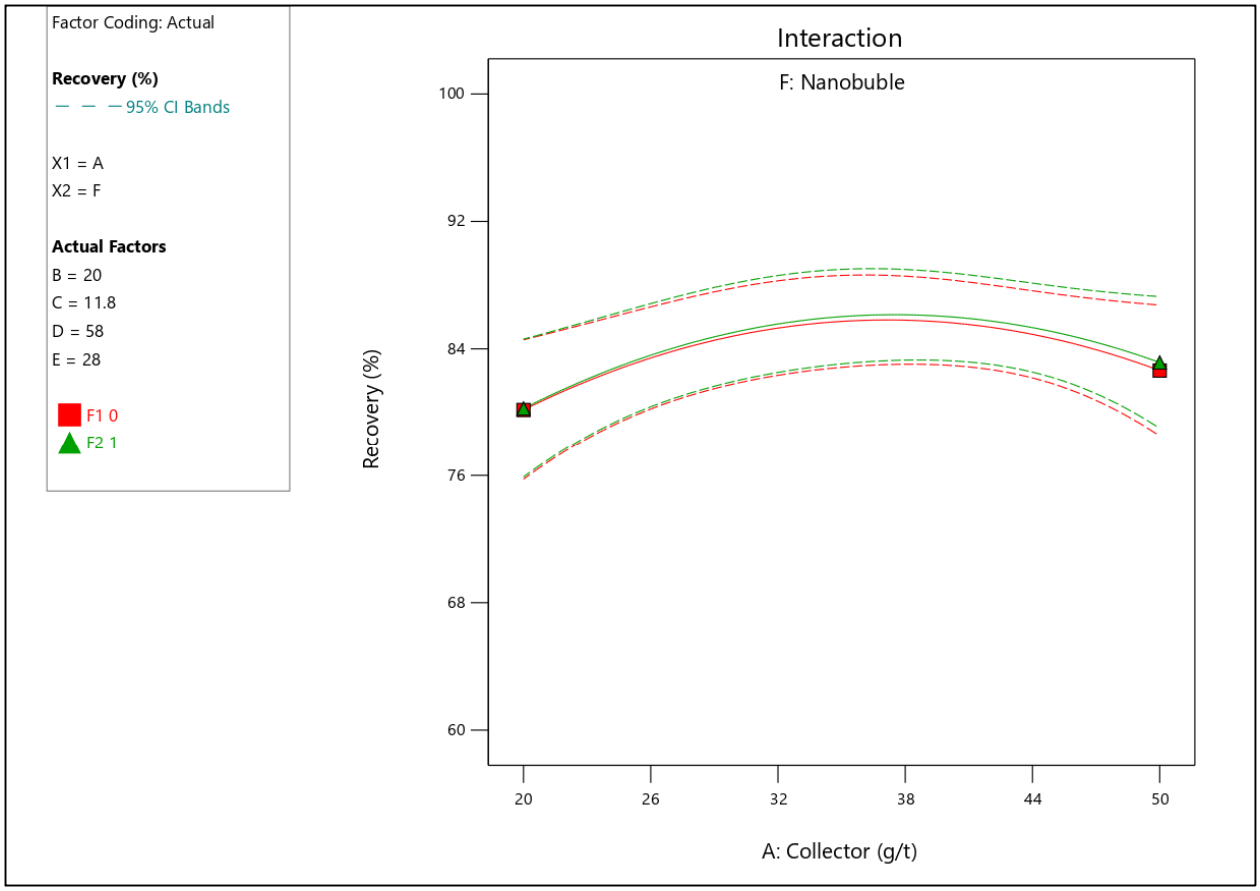

Figure 7. Interactions of the collector on recovery in the presence and absence of nano-microbubbles (B: 20 g/t, C: 11.8, D: 58.5, E: 28).

3.3.2. Effect of frother on recovery in presence and absence of nano-microbubbles

In the absence of nano-microbubbles in Figure 8, it was observed that the higher the amount of frother used in the normal state, the better recovery will be observed. However, in the presence of nano-microbubbles with a lower dosage of frother, better recovery was observed. For example, in the absence of nano-microbubbles, with the consumption of 10 g⁄t of frother, 78.12% recovery was observed while in the presence of nano-microbubbles, 80.05% recovery was obtained, which was a 1.93% increase. The standard consumption limit of the pilot plant of Sarcheshmeh Copper Complex for the frother dosage is 30 g⁄t, where here such a result was obtained with 66.6% less consumption. One of the reasons that can be mentioned why a better recovery was observed with a lower dosage of frother is the good stability of nano-microbubbles.

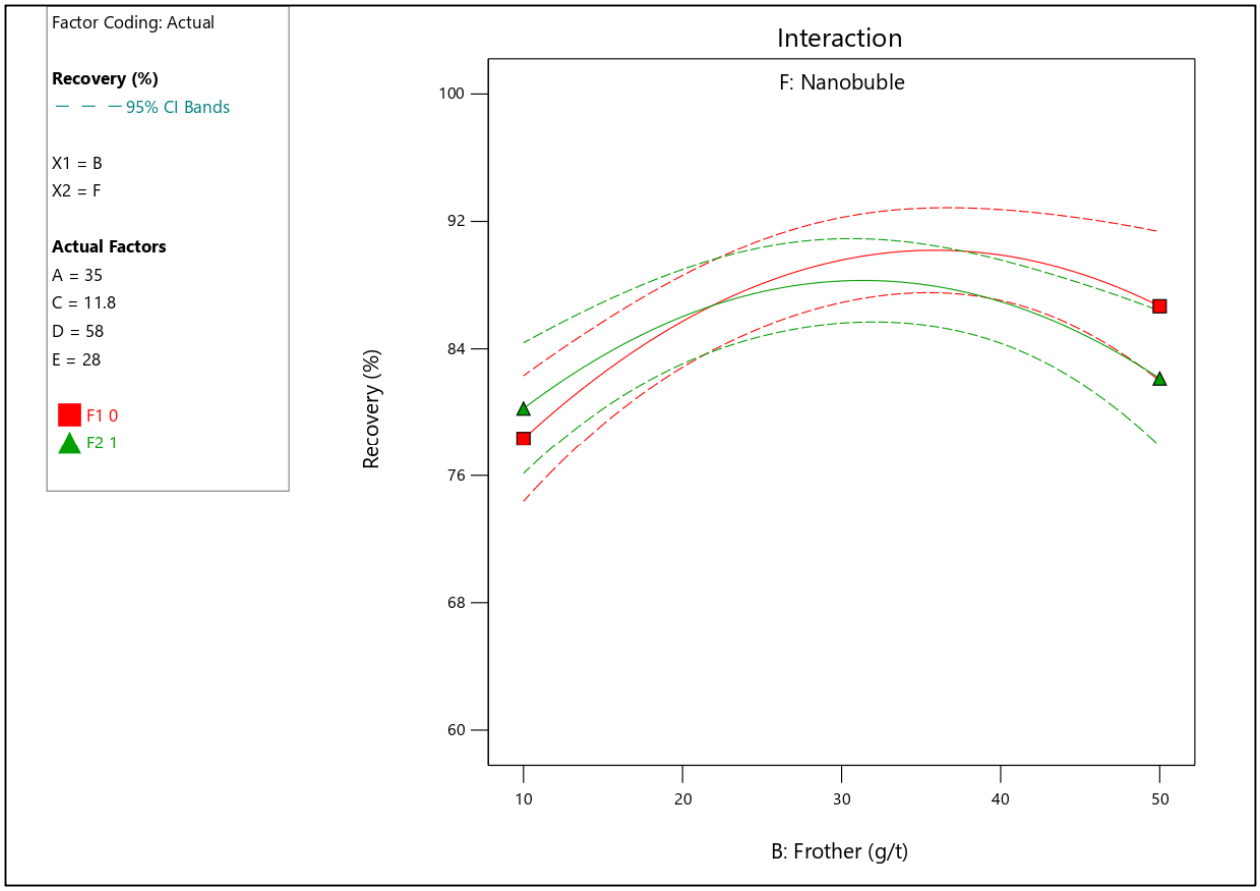

Figure 8. Interaction of frother on recovery in presence and absence of nano-microbubbles (A:35 g/t, C:11.8, D:58.5, E:28).

3.3.3. Effect of pH on recovery in presence and absence of nano-microbubbles

In the absence of nano-microbubbles in Figure 9, better recovery was observed at low pHs. On the contrary, in the presence of nano-microbubbles, the higher the pH of the tests, the better the recovery. The pH in the pilot plant of Sarchemeh Copper Complex is between 11.8 and 12.2. In the experiments conducted from pH 12 to 12.2, better recovery occurred in the presence of nano-microbubbles. At pH 12.2, in the absence of nano-microbubbles, the recovery was 83.45%, and in the presence of nano-microbubbles, the recovery was 86.15%, that is a 2.7% increase was recorded in the presence of nano-microbubbles.

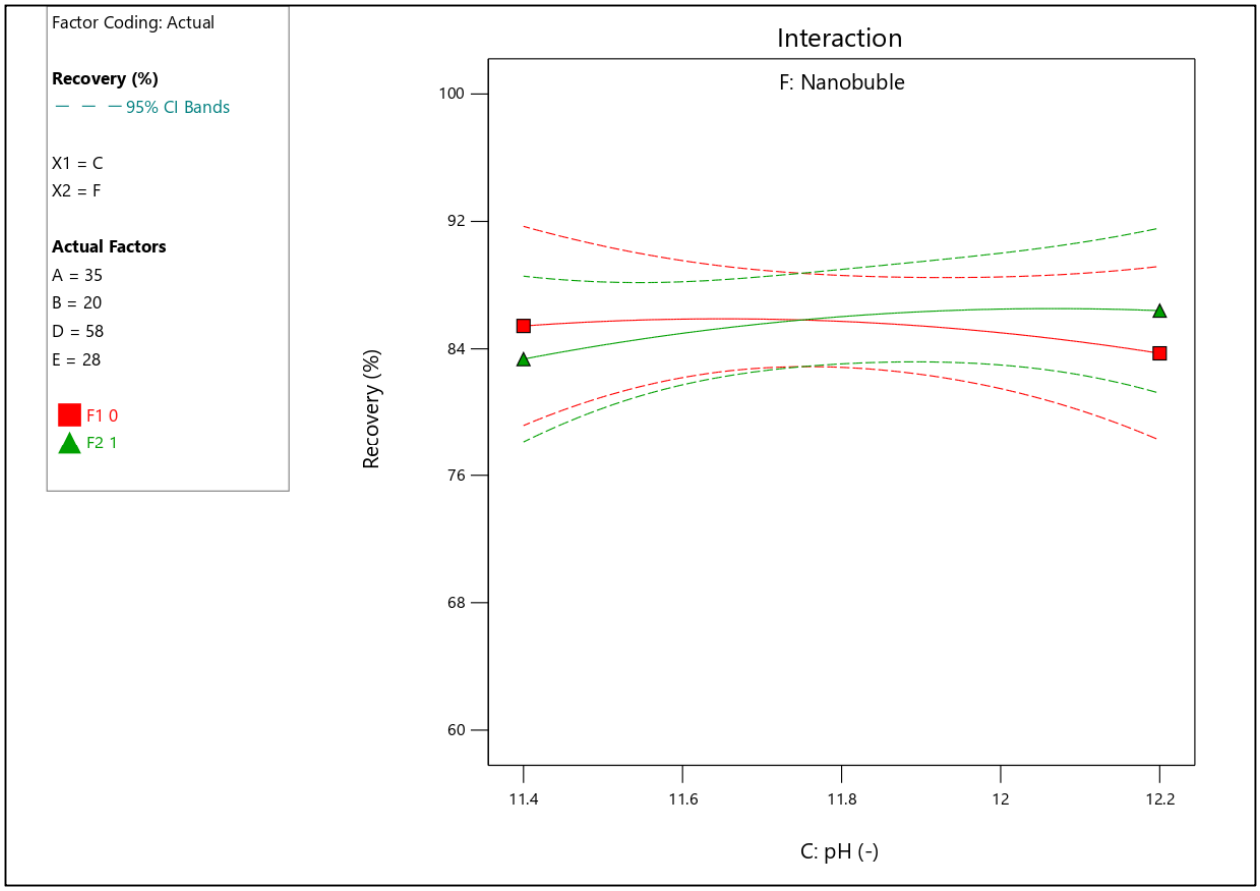

Figure 9. Interaction of pH on recovery in the presence and absence of nano-microbubbles (A:35 g/t, B:20 g/t, D:58.5, E:28).

Zhang *et al.* in 2020 in an article entitled "An experimental study on size distribution and zeta potential of bulk cavitation nanobubbles" have dealt with the reasons why nano-microbubbles have better recovery at high pHs than at lower pHs. They have also studied the effect of pH values on the average size distribution of nanobubbles [59].

3.3.4. Effect of particle size on recovery in absence and presence of nano-microbubbles

As can be seen in Figure 10, in the presence of nano-microbubbles, the interesting thing that was found in this research was that from the dimensions of +50-106 microns, using the variables written below the figure, the recovery in this dimensional range increases which was better than the absence of nano-microbubbles. Perhaps the issue that is raised here is why the nano-microbubbles have not increased in dimensions of 11 microns, which is because if the frother dosage reaches the minimum possible state, i.e. 10 g/t, at that time, with the increase of the collector and the decrease of the frother, the recovery in fine dimensions will increase in proportion to the absence of nano-microbubbles. One of the reasons that can be listed for why nano-microbubbles in dimensions of 106 microns have increased recovery is the fact that there is also fine in coarse dimensions.

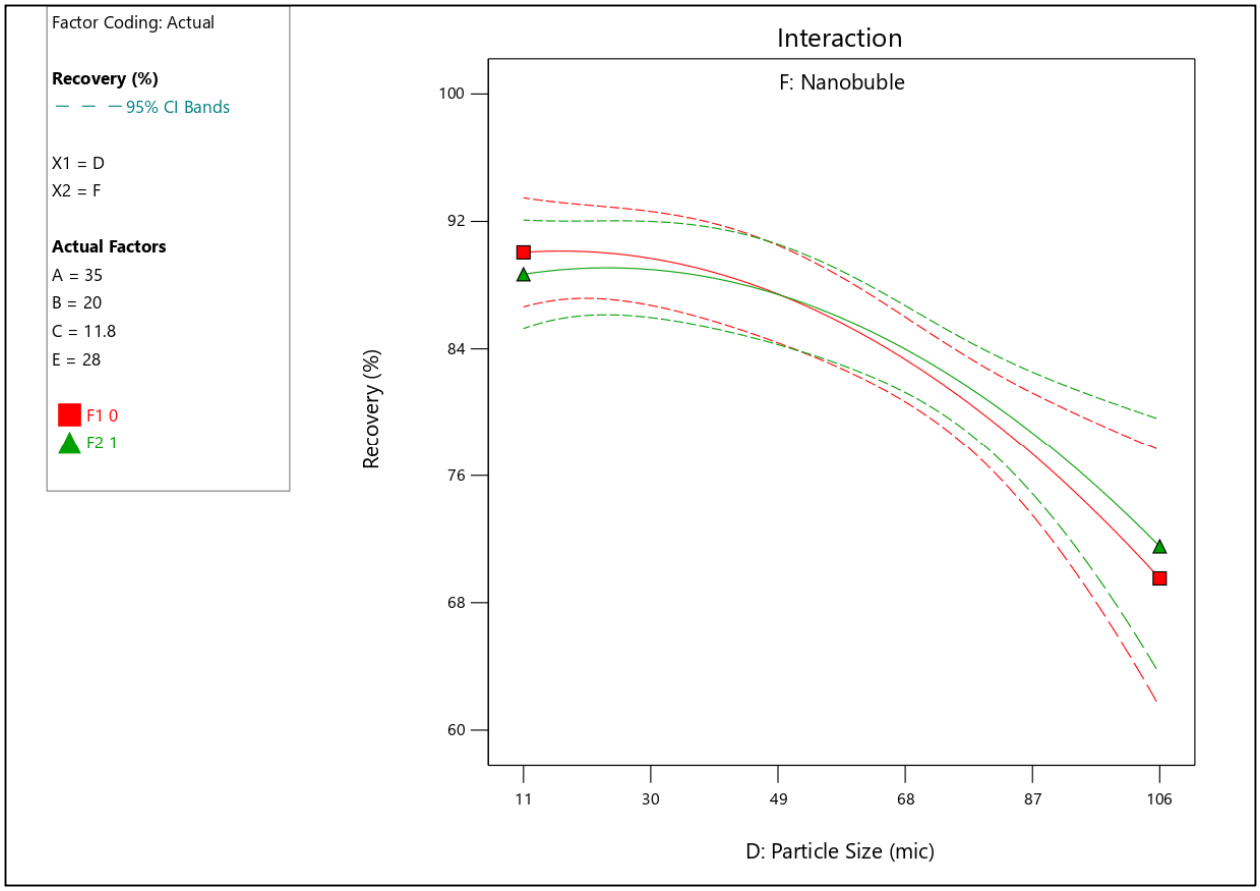

Figure 10. Effect of particle size on recovery in the absence and presence of nano-microbubbles (A:35 g/t, B:20 g/t, C:11.8, E:28).

3.3.5. Effect of solid percentage on recovery in presence and absence of nano-microbubbles

As it can be seen in Figure 11, in the presence of nano-microbubbles with these specific dimensions in the percentage of different solids, compared to the absence of nano-microbubbles, an increase in recovery was observed. One of the reasons that nano-microbubble has given better results in high percentage of solids is that the input soil will increase and naturally the input soft will also increase. The same thing has increased the recovery in high solids percentage compared to low solids percentage. For example, in the solid percentage of 32, in the normal state, 92.64% recovery and in the presence of nano-microbubbles, 94.01% recovery was observed, which has an increase of 1.37% compared to the normal state.

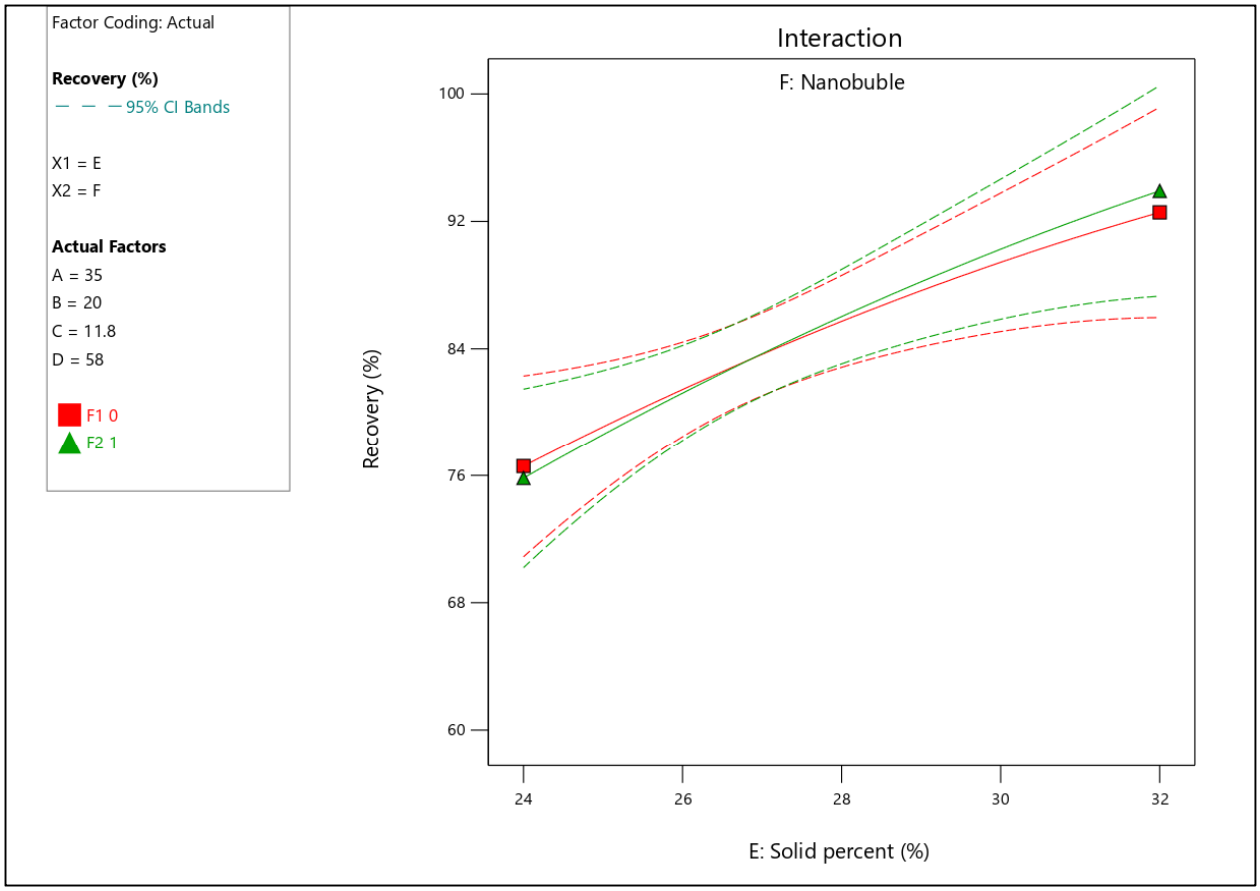

Figure 11. Effect of solid percentage on recovery in the presence and absence of nano-microbubbles (A:35 g/t, B:20 g/t, C:11.8, D:58.5).

3.4. Process optimization

The parameters of the flotation process were optimized using the DX software package and the objective function approach to maximize copper recovery within the experimental range, the results of which are shown in Figure 12. This Figure shows the optimal conditions suggested by the software. It was found that the maximum copper recovery can be obtained around 90.53 with an optimal value of 100% (optimum = 1). The optimal operating conditions suggested by DOE software were: collector dosage 21.35 g/t, frother dosage 10.47 g/t, pH=11.7, particle size 60.5 microns, solid percentage 30.69. Two verification tests were also conducted to validate the proposed model under optimal conditions. The average recovery of two flotation tests was determined to be 88.94%, which indicated the high accuracy of the model.

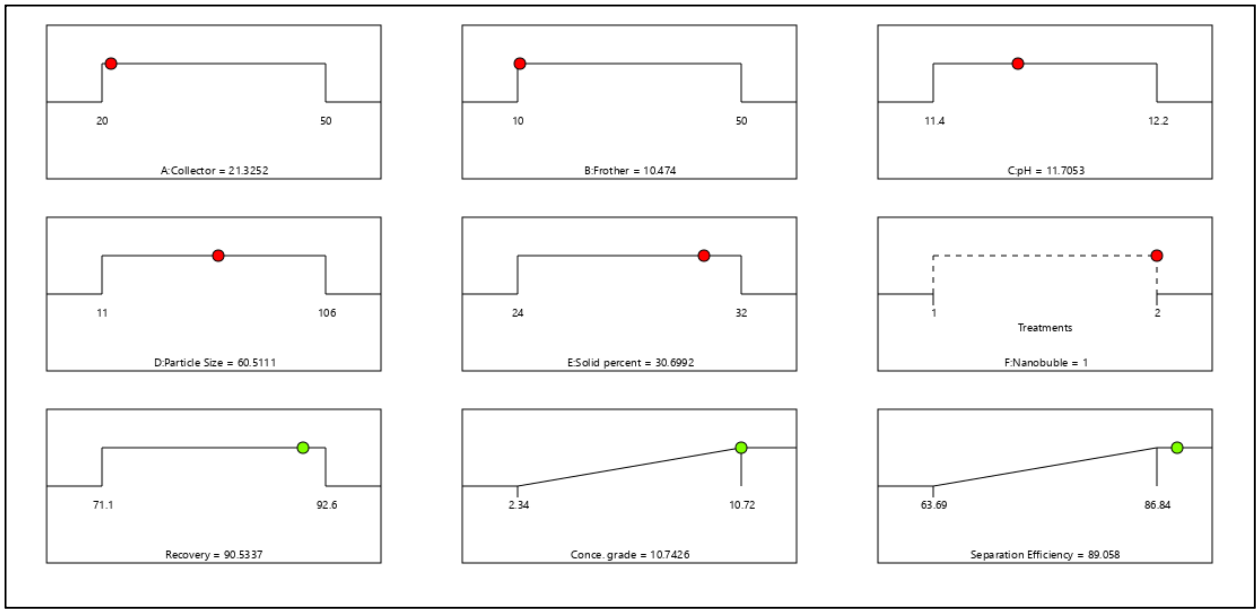

Figure 12. Optimum values of factors to achieve maximum copper recovery.

4. Conclusions

The flotation behavior of Sarcheshmeh copper sulfide rougher was studied by a series of batch flotation experiments. Response surface modeling (RSM) based on central composite design (CCD) was applied to optimize and evaluate the effects of collector dosages, frother dosages, solution pH, particle size, and solid percentage on copper recovery. ANOVA and interaction response surface plots were applied to investigate copper flotation behavior. The main results can be summarized as follows:

1- With less consumption of the collector in the presence of nano-microbubble, the recovery can be increased, the reason is that the nano-microbubble is also used as a secondary collector.

2- One of the reasons that can be mentioned why a better recovery was observed with a lower dosage of frother in the presence of nano-microbubbles is the good stability of nano-microbubbles. Because one of the characteristics of a good frother is its proper stability, which in addition to the frother, nano-microbubble also has this property.

3- One of the reasons that can be mentioned for why nano-microbubbles at high pHs have better recovery than at lower pHs is that the distribution of nano-microbubbles based on volume in pH is considered.

4- In this research work, nano-microbubbles were also effective on coarse copper sulfide particles and increased its recovery compared to the absence of nano-microbubbles.

5- Nano-microbubbles responded better in the percentage of solids of the Sarcheshemeh Copper Complex pilot plant and even higher compared to the percentage of lower solids. One of the reasons is that when the percentage of solids increases, the amount of input soil also increases and therefore there will be more fine materials in the desired soil which makes the nano-microbubbles float them.

Also the following suggestions are made for future research works:

1- It is suggested to investigate the positive and negative effects of nanobubbles in different stages of flotation after the rougher (recleaner, cleaner, and scavenger).

2- Examining the positive and negative effects of nanobubbles on a pilot (semi-industrial) scale

Acknowledgments

The authors express their gratitude to the managers and employees of Sarcheshmeh Copper Complex for their cooperation to carry out this research and also for the permission to publish the article.

References

[1]. Trahar, W. J. (1981). A rational interpretation of the role of particle size in flotation. *International Journal of Mineral Processing*, *8*(4), 289-327.

[2]. Ahmed, N. and Jameson, G. J. (1985). The effect of bubble size on the rate of flotation of fine particles. *International journal of mineral processing*, *14*(3), 195-215.

[3]. Yoon, R. H. and Luttrell, G. H. (1986). The effect of bubble size on fine coal flotation. *Coal Preparation*, *2*(3), 179-192.

[4]. Ding, S., Xing, Y., Zheng, X., Zhang, Y., Cao, Y., and Gui, X. (2020). New insights into the role of surface nanobubbles in bubble-particle detachment. *Langmuir*, *36*(16), 4339-4346.

[5]. Lei, W., Zhang, M., Zhang, Z., Zhan, N., and Fan, R. (2020). Effect of bulk nanobubbles on the entrainment of kaolinite particles in flotation. *Powder Technology*, *362*, 84-89.

[6]. Liu, L., Hu, S., Wu, C., Liu, K., Weng, L., and Zhou, W. (2021). Aggregates characterizations of the ultra-fine coal particles induced by nanobubbles. *Fuel*, *297*, 120765.

[7]. Tao, D., Wu, Z., and Sobhy, A. (2021). Investigation of nanobubble enhanced reverse anionic flotation of hematite and associated mechanisms. *Powder Technology*, *379*, 12-25.

[8]. Zhou, W., Chen, H., Ou, L., and Shi, Q. (2016). Aggregation of ultra-fine scheelite particles induced by hydrodynamic cavitation. *International Journal of Mineral Processing*, *157*, 236-240.

[9]. Zhou, W., Niu, J., Xiao, W., and Ou, L. (2019). Adsorption of bulk nanobubbles on the chemically surface-modified muscovite minerals. *Ultrasonics Sonochemistry*, *51*, 31-39.

[10]. Matis, K. A., Gallios, G. P., and Kydros, K. A. (1993). Separation of fines by flotation techniques. *Separations Technology*, *3*(2), 76-90.

[11]. Ansari, M. I. (1997). Fine particle processing-A difficult problem for mineral engineers.

[12]. Yalcin, T. and Byers, A. (2006). Dissolved gas flotation in mineral processing. *Mineral Processing and Extractive Metallurgy Review*, *27*(2), 87-97.

[13]. Maoming, F. A. N., Daniel, T. A. O., Honaker, R., and Zhenfu, L. U. O. (2010). Nanobubble generation and its applications in froth flotation (part III): specially designed laboratory scale column flotation of phosphate. *Mining Science and Technology (China)*, *20*(3), 317-338.

[14]. Maoming, F. A. N., Daniel, T. A. O., HONAKER, R., and Zhenfu, L. U. O. (2010). Nanobubble generation and its applications in froth flotation (part IV): mechanical cells and specially designed column flotation of coal. *Mining Science and Technology (China)*, *20*(5), 641-671.

[15]. Jameson, G. J. (2010). Advances in fine and coarse particle flotation. *Canadian Metallurgical Quarterly*, *49*(4), 325-330.

[16]. Ushikubo, F. Y., Furukawa, T., Nakagawa, R., Enari, M., Makino, Y., Kawagoe, Y., ... and Oshita, S. (2010). Evidence of the existence and the stability of nano-bubbles in water. *Colloids and Surfaces A: Physicochemical and Engineering Aspects*, *361*(1-3), 31-37.

[17]. Miettinen, T., Ralston, J., and Fornasiero, D. (2010). The limits of fine particle flotation. *Minerals engineering*, *23*(5), 420-437.

[18]. Albijanic, B., Amini, E., Wightman, E., Ozdemir, O., Nguyen, A. V., and Bradshaw, D. J. (2011). A relationship between the bubble–particle attachment time and the mineralogy of a copper–sulphide ore. *Minerals Engineering*, *24*(12), 1335-1339.

[19]. Albijanic, B., Bradshaw, D. J., and Nguyen, A. V. (2012). The relationships between the bubble–particle attachment time, collector dosage and the mineralogy of a copper sulfide ore. *Minerals Engineering*, *36*, 309-313.

[20]. Calgaroto, S., Wilberg, K. Q., and Rubio, J. (2014). On the nanobubbles interfacial properties and future applications in flotation. *Minerals Engineering*, *60*, 33-40.

[21]. Mazahernasab, R. and Ahmadi, R. (2016). Determination of bubble size distribution in a laboratory mechanical flotation cell by a laser diffraction technique. *Physicochemical Problems of Mineral Processing*, *52*.

[22]. Leistner, T., Peuker, U. A., and Rudolph, M. (2017). How gangue particle size can affect the recovery of ultrafine and fine particles during froth flotation. *Minerals Engineering*, *109*, 1-9.

[23]. Rulyov, N., Nessipbay, T., Dulatbek, T., Larissa, S., & and Zhamikhan, K. (2018). Effect of microbubbles as flotation carriers on fine sulphide ore beneficiation. *Mineral Processing and Extractive Metallurgy*, *127*(3), 133-139.

[24]. Nazari, S., Shafaei, S. Z., Gharabaghi, M., Ahmadi, R., Shahbazi, B., and Maoming, F. (2019). Effects of nanobubble and hydrodynamic parameters on coarse quartz flotation. *International Journal of Mining Science and Technology*, *29*(2), 289-295.

[25]. de Medeiros, A. R. S. and Baltar, C. A. M. (2018). Importance of collector chain length in flotation of fine particles. *Minerals Engineering*, *122*, 179-184.

[26]. Tao, D. and Sobhy, A. (2019). Nanobubble effects on hydrodynamic interactions between particles and bubbles. *Powder technology*, *346*, 385-395.

[27]. Ebrahimi, H., Karamoozian, M., and Saghravani, S. F. (2022). Interaction of applying stable micro-nano bubbles and ultrasonic irradiation in coal flotation. *International Journal of Coal Preparation and Utilization*, *42*(5), 1548-1562.

[28]. Farrokhpay, S., Filippova, I., Filippov, L., Picarra, A., Rulyov, N., and Fornasiero, D. (2020). Flotation of fine particles in the presence of combined microbubbles and conventional bubbles. *Minerals Engineering*, *155*, 106439.

[29]. Farrokhpay, S., Filippov, L., and Fornasiero, D. (2021). Flotation of fine particles: A review. *Mineral Processing and Extractive Metallurgy Review*, *42*(7), 473-483.

[30]. Li, C., Xu, M., Xing, Y., Zhang, H., and Peuker, U. A. (2020). Efficient separation of fine coal assisted by surface nanobubbles. *Separation and Purification Technology*, *249*, 117163.

[31]. Chang, G., Xing, Y., Zhang, F., Yang, Z., Liu, X., and Gui, X. (2020). Effect of nanobubbles on the flotation performance of oxidized coal. *ACS omega*, *5*(32), 20283-20290.

[32]. Nazari, S. and Hassanzadeh, A. (2020). The effect of reagent type on generating bulk sub-micron (nano) bubbles and flotation kinetics of coarse-sized quartz particles. *Powder Technology*, *374*, 160-171.

[33]. Sobhy, A., Wu, Z., and Tao, D. (2021). Statistical analysis and optimization of reverse anionic hematite flotation integrated with nanobubbles. *Minerals Engineering*, *163*, 106799.

[34]. Zhang, Z., Ren, L., and Zhang, Y. (2021). Role of nanobubbles in the flotation of fine rutile particles. *Minerals Engineering*, *172*, 107140.

[35]. Li, C. and Zhang, H. (2022). A review of bulk nanobubbles and their roles in flotation of fine particles. *Powder Technology*, *395*, 618-633.

[36]. Li, C. and Zhang, H. (2022). Surface nanobubbles and their roles in flotation of fine particles–A review. *Journal of Industrial and Engineering Chemistry*, *106*, 37-51.

[37]. Schubert, H. (2005). Nanobubbles, hydrophobic effect, heterocoagulation and hydrodynamics in flotation. *International Journal of Mineral Processing*, *78*(1), 11-21.

[38]. Hampton, M. A. and Nguyen, A. V. (2009). Systematically altering the hydrophobic nanobubble bridging capillary force from attractive to repulsive. *Journal of colloid and interface science*, *333*(2), 800-806.

[39]. Montgomery, D. C. (2001). Design and analysis of experiments. John Wiley & Sons. *Inc., New York*, *1997*, 200-1.

[40]. Myers, R. H., Montgomery, D. C., and Anderson-Cook, C. M. (2016). *Response surface methodology: process and product optimization using designed experiments*. John Wiley & Sons.

[41]. Hinkelman, K., Kempthorne, O., and Kshivsagar, A. M. (1996). Design and analysis of experiments. Volume I: Introduction to experimental design. *Statistical Methods in Medical Research*, *5*(1), 101-101.

[42]. Kincl, M., Turk, S., and Vrečer, F. (2005). Application of experimental design methodology in development and optimization of drug release method. *International journal of pharmaceutics*, *291*(1-2), 39-49.

[43]. Simate, G. S., Ndlovu, S., and Gericke, M. (2009). Bacterial leaching of nickel laterites using chemolithotrophic microorganisms: process optimisation using response surface methodology and central composite rotatable design. *Hydrometallurgy*, *98*(3-4), 241-246.

[44]. Niaki, R., Abazarpoor, A., Halali, M., Maarefvand, M., and Ebrahimi, G. (2015). Application of response surface methodology and central composite rotatable design for modeling and optimization of sulfuric and nitric leaching of spent catalyst. *Russian Journal of Non-Ferrous Metals*, *56*, 155-164.

[45]. Behera, S. K., Meena, H., Chakraborty, S., and Meikap, B. C. (2018). Application of response surface methodology (RSM) for optimization of leaching parameters for ash reduction from low-grade coal. *International Journal of Mining Science and Technology*, *28*(4), 621-629.

[46]. Sahu, J. N., Acharya, J., and Meikap, B. C. (2009). Response surface modeling and optimization of chromium (VI) removal from aqueous solution using Tamarind wood activated carbon in batch process. *Journal of hazardous materials*, *172*(2-3), 818-825.

[47]. Vazifeh, Y., Jorjani, E., and Bagherian, A. (2010). Optimization of reagent dosages for copper

flotation using statistical technique. *Transactions of Nonferrous Metals Society of China*, *20*(12), 2371-2378.

[48]. Rao, G. V. and Mohanty, S. (2002). Optimization of flotation parameters for enhancement of grade and recovery of phosphate from low-grade dolomitic rock phosphate ore from Jhamarkotra, India. *Mining, Metallurgy & Exploration*, *19*, 154-160.

[49]. Aslan, N. E. V. Z. A. T. and Fidan, R. (2008). Optimization of Pb flotation using statistical technique and quadratic programming. *Separation and Purification Technology*, *62*(1), 160-165.

[50]. Mehrabani, J. V., Noaparast, M., Mousavi, S. M., Dehghan, R., and Ghorbani, A. (2010). Process optimization and modelling of sphalerite flotation from a low-grade Zn-Pb ore using response surface methodology. *Separation and Purification Technology*, *72*(3), 242-249.

[51]. Kwak, J. S. (2005). Application of Taguchi and response surface methodologies for geometric error in surface grinding process. *International journal of machine tools and manufacture*, *45*(3), 327-334.

[52]. Awe, S. A., Khoshkhoo, M., Kruger, P., and SANDSTROeM, A. (2012). Modelling and process optimisation of antimony removal from a complex copper concentrate. *Transactions of Nonferrous Metals Society of China*, *22*(3), 675-685.

[53]. Bezerra, M. A., Santelli, R. E., Oliveira, E. P., Villar, L. S., and Escaleira, L. A. (2008). Response surface methodology (RSM) as a tool for optimization in analytical chemistry. *Talanta*, *76*(5), 965-977.

[54]. Rakić, T., Kasagić-Vujanović, I., Jovanović, M., Jančić-Stojanović, B., and Ivanović, D. (2014). Comparison of full factorial design, central composite design, and box-behnken design in chromatographic method development for the determination of fluconazole and its impurities. *Analytical Letters*, *47*(8), 1334-1347.

[55]. Box, G. E. and Hunter, J. S. (1957). Multi-factor experimental designs for exploring response surfaces. *The Annals of Mathematical Statistics*, 195-241.

[56]. Kafshgari, L. A., Ghorbani, M., Azizi, A., Agarwal, S., and Gupta, V. K. (2017). Modeling and optimization of Direct Red 16 adsorption from aqueous solutions using nanocomposite of MnFe2O4/MWCNTs: RSM-CCRD model. *Journal of molecular liquids*, *233*, 370-377.

[57]. Arefi, A. **(**2015). Application of micro/nanobubbles and nanomaterials in improving the mechanical behavior and insulation of building materials (with emphasis on concrete**).** Master of Science Thesis in Civil Engineering (Water and Environment), Faculty of Civil Engineering, Shahrood University of Technology, Shahrood, Iran.

[58]. Tao, Y., Liu, J., Yu, S., and Tao, D. (2006). Picobubble enhanced fine coal flotation. *Separation Science and Technology*, *41*(16), 3597-3607.

[59]. Zhang, X. Y., Wang, Q. S., Wu, Z. X., and Tao, D. P. (2020). An experimental study on size distribution and zeta potential of bulk cavitation nanobubbles. *International Journal of Minerals, Metallurgy and Materials*, *27*, 152-161.

تأثیر نانو-میکروحباب‌های پایدار بر فلوتاسیون مس سولفیدی و کاهش میزان مصرف مواد شیمیایی

علی نیکوئی ماهانی[1]، محمد کارآموزیان[1]، محمد جهانی چگنی[1*] و محمد محمودی میمند[2]

1. دانشکده مهندسی معدن، نفت و ژئوفیزیک، دانشگاه صنعتی شاهرود، شاهرود، ایران

2. بخش تحقیق و توسعه، معدن مس سرچشمه، شرکت ملی صنایع مس ایران، رفسنجان، ایران

ارسال 2023/06/01، پذیرش 2023/07/16

* نویسنده مسئول مکاتبات: M.Jahani@shahroodut.ac.ir

چکیده:

به طور کلی کارخانه‌های فرآوری مواد معدنی مقدار زیادی باطله در قالب ذرات نرمه ایجاد می‌کنند. سرعت فلوتاسیون میکروحباب‌های معدنی توسط حباب‌های درشت چندین برابر در مقایسه با سرعت فلوتاسیون ذرات جداگانه است. مزیت میکروحباب‌ها به دلیل افزایش کارایی اتصال حباب‌های معمولی با ذرات ریز پوشیده شده از میکروحباب‌ها می‌باشد. در این جا تمرکز بر کاهش مصرف مواد شیمیایی و افزایش بازیابی است. پس از تهیه نمونه معرف، آنالیزهای XRF، XRD و کانی شناسی انجام شدند. سپس، با طراحی آزمایش به روش سطح پاسخ و با طراحی مرکب مرکزی توسط نرم‌افزار DX13، 50 آزمایش انجام شدند. تاثیر متقابل پارامترها شامل مقدار مصرف کلکتور، کف‌ساز، pH، اندازه ذرات و درصد جامد بررسی شدند. 25 آزمایش با فلوتاسیون معمولی و 25 آزمایش تحت تاثیر نانومیکروحباب‌ها انجام شدند. حد استاندارد آزمایشگاهی کلکتور مصرفی در پایلوت پلنت مجتمع مس سرچشمه 40 گرم بر تن است (25 گرم بر تن C7240 بعلاوه 15 گرم بر تن Z11). در اینجا با مصرف 20 گرم بر تن کلکتور در عدم حضور نانومیکروحباب‌ها، بازیابی 79/96 بدست آمد و در حضور نانومیکروحباب‌ها، بازیابی 80/07 درصد بدست آمد. یعنی کاهش50 درصدی در مصرف کلکتور و افزایش 0/11 درصدی در بازیابی مشاهده شد. همچنین، حد استاندارد آزمایشگاهی کف‌ساز مصرفی در پایلوت پلنت مجتمع مس سرچشمه 30 گرم بر تن است (15 گرم بر تن MIBC بعلاوه 15 گرم بر تنA65). در اینجا با مصرف 10 گرم بر تن کف‌ساز در عدم حضور نانومیکروحباب‌ها، بازیابی 78/12 درصد بدست آمد و در حضور نانومیکروحباب‌ها بازیابی 82/05 درصد بدست آمد. به عبارت دیگر، کاهش 66/6 درصدی در مصرف کف‌ساز و افزایش 1/93درصدی در بازیابی مشاهده شد.

کلمات کلیدی: نانومیکروحباب‌های پایدار، تاثیر متقابل، طراحی آزمایش، میزان مصرف مواد شیمیایی، بازیابی.